Digital Light Processing Stereolithography and Si(O)C Manufacturing

Sébastien Vry[a], Marilyne Roumanie[a], Guillaume Bernard-Granger[b], Richard Laucournet[a]

[a]*Université Grenoble Alpes, CEA, LITEN, DTNM, Grenoble,38000, France*

[b]*CEA, Nuclear Energy Division, Research Department on Mining and Fuel Recycling Processes, 30207 Bagnols-sur-Cèze, France*

1. Abstract

Silicon carbide (SiC) is a high performance ceramic used in high temperature environments (refractory, brakes, turbine engines…), power devices and modules. Stereolithography processing can lead to complex shape ceramic parts compared to conventional ceramic processes. However, SiC powder strongly absorbs the UV light, inhibiting the resin photopolymerization reaction. Polysiloxane and polycarbosilane are preceramic polymers leading to Si(O)C ceramics. These polymers are consistent with UV processing and offer the possibility to process carbides by stereolithography. The investigations on the development of UV-curable formulation with preceramic polymer suitable for SLA process and the composition of the final material are reported in this paper.

2. Introduction

Research on technical ceramics in automotive, aerospace and aviation revealed that silicon carbide (SiC) ceramics fulfil the demand for high temperature resistance and lightweight structures. Shaping SiC by a conventional powder metallurgy approach of ceramic powder leading to a dense material with high mechanical properties is obtained by pressing, machining and sintering at high temperature (1800 - 2000°C). The machining step is therefore expensive and geometries addressed are limited. Additive manufacturing (AM) processes offer the opportunity to manufacture complex parts. Among AM, the stereolithography (SLA) process based on photocurable resins is known to shape complex ceramics parts[1]. However, SiC powder absorbs the UV light, inhibiting the resin photopolymerization, even for low solid loadings (< 10% vol) [2].

Preceramic polymers such as polysilazane, polycarbosilane and polysiloxane are silicon-based polymers leading to a wide range of chemical compositions[3] after pyrolysis: SiCN, SiOC, SiC or quaternary systems are achievable, as examples. These ceramics are referred as Polymer-Derived Ceramics (PDC). Recently AM technologies such as selective laser curing[4], inkjet printing[5], and SLA[6–12] were applied to preceramic polymers. The main advantages of these polymers are a lower light-absorbance than raw SiC powder, a miscibility in photocurable resins and a low processing temperature (1000-1700°C) compared to a standard powder-based sintering approach (1800-2000°C). However, the high weight loss and shrinkage occurring during the conversion step of the polymer formulation to ceramic may lead to extensive cracks generation. Polycarbosilane polymers are the suitable candidates to target a SiC material. These organometallic polymers are expensive and oxygen sensitive. Polysiloxanes polymers are an alternative to overcome the issue and simplify the handling procedures.

In the stereolithography process, the approach of blending a high ceramic yield polymer with a photocurable resin was reported in literature[11]. This approach do not need any complex synthesis such as modification of preceramic polymers into a photosensitive oligomer. The blending approach enlarges the range of precursors usable.

The main technical issues to suit SLA requirements and to obtain after an appropriate thermal treatment the highest amount of ceramic phase are listed below:

- Achieving high loadings of preceramic polymer in the photocurable resin,
- Manufacture parts with a thickness layer around 100μm;
- Formulating a stable blend over the manufacturing time.

The objectives of the work presented in this paper are: (a) to investigate the thermal behaviour of the commercial polysiloxane Silres H62C followed by chemical and microstructure analysis from 1000°C to 1700°C; (b) to develop a photocurable PDC resin suitable with the DLP printing process, (c) to compare the final SiOC material obtained by DLP and the raw Silres H62C obtained after thermal treatments.

3. **Materials and methods**

Formulation

This work focuses on using commercial methylphenylvinylhydrogen polysiloxane as a preceramic polymer (Silres H62C, Wacker-Chemie AG). This preceramic polymer is liquid at room temperature and contains a platinum complex catalyst. The cross-linking of the Silres H62C occurs through a polyaddition of vinyl groups and a hydrosilylation related to the presence of silyl (Si-H) groups. The cross-linking range temperature is between 195 and 260°C with a maximum of curing at 200°C. Pt-complex catalyst ensures a low curing temperature. In the following, the cross-linked Silres H62C will be noted Silres H62C-c.

Two photosentive resins, noted F1 and F2, were investigated and described below. The F1 resin is a blend of 1,6-hexanediol diacrylate (SR238 – Sartomer) and a photoinitiator (PI). Four PIs were investigated according to their effect on the cured thickness after UV irradiance: Phenylbis (2, 4, 6-trimethylbenzoyl) phosphine oxide (PI-819 - Sigma Aldrich), 2-Benzyl-2-(diméthylamino)-4'-morpholinobutyrophénone (PI-369 - Sigma Aldrich), 2,2-Dimethoxy-2-phenylacetophenone (PI-651 - Sigma Aldrich) and Diphenyl(2,4,6-trimethylbenzoyl)phosphine oxide (PI-TPO, BASF). The PI content is fixed at 1 mol.% and 2 mol. % related to the organic resin.

F2 resin is a blend of 1, 6 hexanediol-diacrylate (HDDA, SR238 Sartomer, Arkema) with polyethyleneglycol diacrylate (PEG250DA, Sigma Aldrich) with the 1:1 ratio. 0.6wt% of PI-819 photoinitiator is dissolved in the resin. To limit the UV penetration depth[9,12,13] and decrease the polymerized thickness, organic dyes photoabsorber were added to the resin. The investigations were focused on the Benzene-1-azo-2-naphthol (Sudan I, Sigma Aldrich), the 2,5-Bis(5-tert-butyl-benzoxazol-2-yl)thiophene (BBOT, Sigma Aldrich) and the Copper(II) phthalocyanine (Cu(II)PC, Sigma Aldrich) as photoabsorbers. The addition of PEGDA in F2 ensures the dissolution of organic photoabsorbers. For F1 and F2 resins, Silres H62C was blended with photocurable resin with a 3:1 ratio.

Table 1 summarises the compositions of the PDC photosensitive formulations retained.

Photocurable formulation	H62C (wt %)	Acrylate base (ratio)	Photoinitiator	Photoabsorber
PDC-F1	75	SR238	1 mol.% or 2 mol.%	-
PDC-F2	75	SR238-PEGDA (1:1)	PI-819 – 0.6 mol.%	0.1-0.4 mol.%

Table 1: F1 and F2 formulations. Photoinitiator and photoabsorber contents are expressed in mol % relative to the acrylate amount.

PDC formulation curing behavior

To assess the ability to print structures, the curing thickness is measured related to the curing time. An UV light head prints a square pattern, then the cured layer is cleaned with Di(propylene glycol) methyl ether (Sigma Aldrich) and finally the thickness is measured in 5 spots with an ultrasonic coating thickness gauge (Elcometer 355 F1 standard probe 0 - 1500 µm with a ferrous zero plate) (Fig. 1). The thickness target is between 100 and 200 µm for an irradiance of 88 mW/cm².
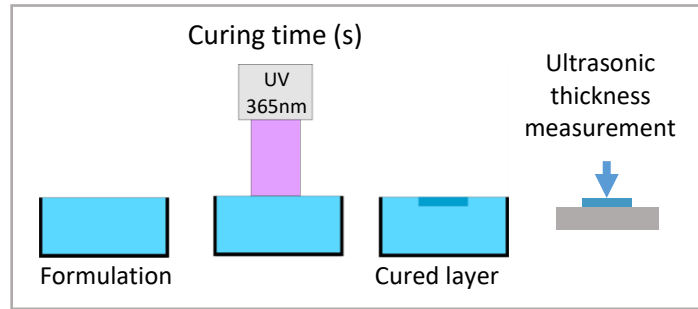

Fig. 1 Cured mono-layer to measure thickness versus curing time

SLA process

Printing structures was constructed with F2 photocurable formulation using a Digital Light Processing Stereolithography equipment (M120 Prodways). The top-down operating approach is described in Fig. 2. From a CAD model, the parts are printed layer-wise. The platform dip into the vat of resin and then the DLP, with UV LED at 365nm, projects a pattern onto the liquid surface. The photocured layers are then immersed into the liquid and a new layer is spread on top of the previous one. The process is carried on until the 3D part is built by stacking the polymerized layers. A post curing is commonly performed through a heat treatment or an UV-irradiation to cure remaining monomers. The DLP source irradiance is set to 88 mW/cm².

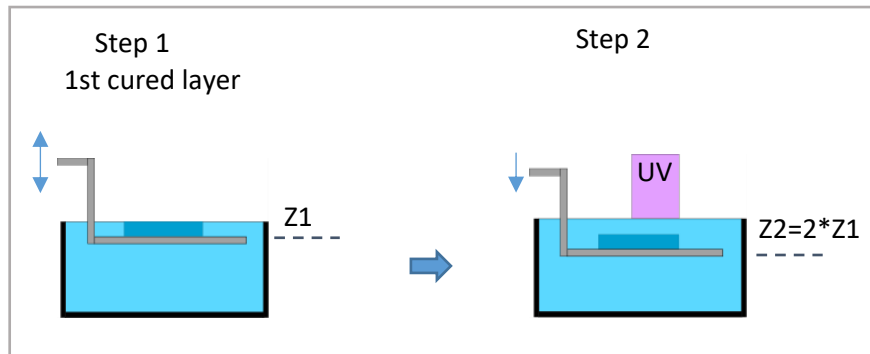*Fig. 2 Stereolithography process with top-down approach*

Thermal cycle

Following the photocuring stage, the preceramic polymer is trapped into the 3D network of the photosensitive resin. To crosslink the preceramic polymer and increase the ceramic yield after pyrolysis, parts are cured in air at 200°C, during 1h, with a heating ramp of 0.1 K/min. Then samples and 3D structures are positioned on a flat amorphous carbon crucible and pyrolyzed in argon, at 1000°C, during 1h, with a heating ramp fixed to 1K/min.

3.2 Characterizations

Chemical analysis

The crystallization behaviour of pyrolyzed ceramics at 1000, 1400 and 1700°C in argon were monitored by X-ray diffraction (XRD, Bruker D8 Advance, LynxEye detector with Cu-Kα radiation) with 2θ values ranging from 10 to 90° (step 0.05 and counting time of 1s at each position). EVA Software and JCPDS (*Joint Committee on Powder Diffraction Standards*) database were used to identify the crystalline phases regarding the resolution limit of the equipment.

Analyses of carbon, oxygen and hydrogen contents were performed by Instrumental Gas Analysis (IGA, Carbon-ISO15350, Oxygen-DIN EN 10276, Hydrogen-DIN EN 10720). Silicon content was measured by Inductively Coupled Plasma atomic emission spectroscopy (ICP, DIN 51008-2 & DIN 51009).

Transmission Electron Microscopy (TEM) observations were done using a Tecnai Osiris (FEI, Eindhoven, Netherlands, acceleration voltage of 200 kV, point to point resolution of 2.5 Å). Thin foils were prepared using focus ion beam.

Real-Time Infrared Spectroscopy (RT-FTIR)

The photo-curing behaviour (polymerization profile, final conversion, polymerization rate and inhibition time) was determined by RT-FTIR measurements. The sample was exposed simultaneously to UV irradiation with an UV-LED unit (LC-L1V5, 365nm, Hamamatsu photonics) and to the the IR beam of the spectrophotometer (Vertex 70, Bruker) equipped with a time resolved detector (MCT, Bruker - Spectral resolution 4 cm^{-1} with 8-10 scans/s acquisition speed). The photocurable formulation was deposited onto a polypropylene film (PP30, thickness 30µm, Good Fellow) with a calibrated wire wound bar coater. The film thickness was set to 20 µm and the surface was covered with the same polypropylene film to overcome oxygen inhibition. The irradiance of the UV source was set between 15 and 88 mW/cm². The polymerization profiles were recorded by monitoring the decay of the absorption bands of the acrylate double bonds at 1410 cm^{-1} and 1636 cm^{-1}. From the first derivative of the polymerization profiles, the polymerization rate can be calculated according to $Rp = -\frac{d[M]}{dt}$ where [M] is the monomer concentration. The maximum rate of polymerization $\left(\frac{Rp}{[M]_0}\right)_{max}$ is then determined by taking the maximum slope of the polymerization curve.

4. Results and Discussion

4.1 Polymer to ceramic conversion at high temperature

The weight loss of pure and cross-linked polysiloxane Silres H62C (Silres H62C-c) between room temperature and 1000°C in argon are shown in Fig. 3 (a). Total weight loss of pure Silres H62C is 30.4 wt. %, meaning that the ceramic SiO_xC_y yield is 69.6 wt. %. The crosslinking of the Silres H62C lead to a volatile burnout and the development of a polysiloxane 3D network. The chemical rearrangement of the Silres H62C- c increases the ceramic yield[14] of 3 wt. %.

Silres H62C-c pyrolyzed at 1000, 1400 and 1700°C in argon were investigated with respect to their crystalline phase composition by XRD, Fig. 3 (b). After pyrolysis at 1000°C, an amorphous X-ray diffraction signal is detected, characterized by a broad hump positioned at $2\theta = 20.6°$. This signal indicates the presence of bonding between Si and O in an amorphous state. It was only at 1400°C that crystallisation starts, with the presence of first specific diffraction peaks of SiC, localised at $2\theta = 35.6°$, 59.9°, 71.7. After pyrolysis at 1700°C, the intensity of reflections increased significantly and confirms the presence of crystallised β-SiC (3C-SiC). The reflexion at around $2\theta = 33.6°$ indicates the presence of α-SiC phase and/or stacking faults in the 3C-SiC structure[15].
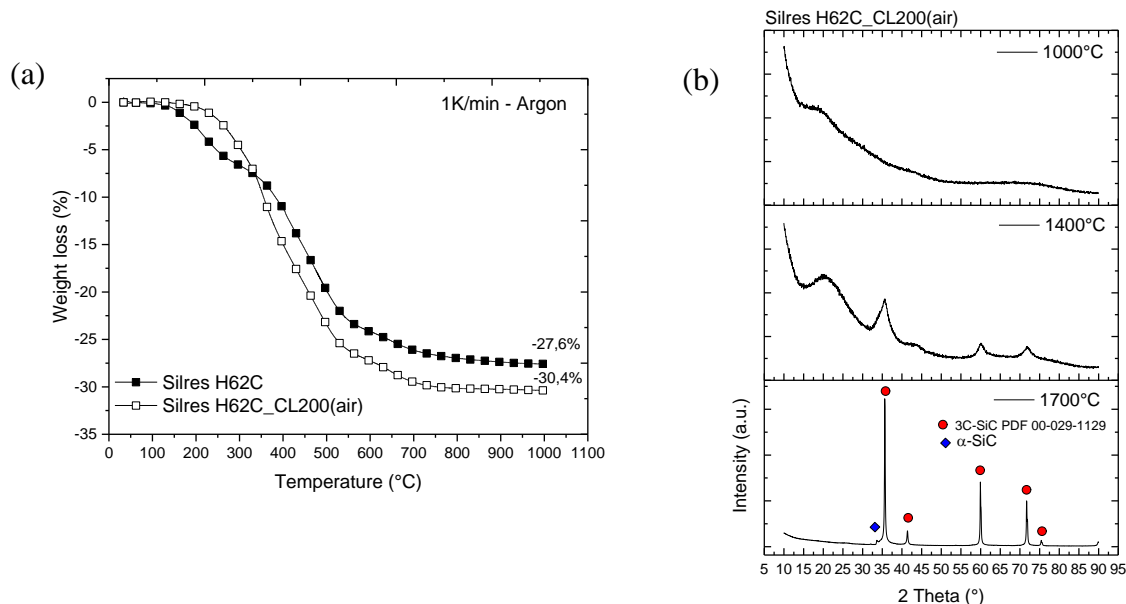

Fig. 3 (a) TGA of pure and crosslinked Silres H62C at 200°C in air during 1h. (b) XRD analysis of H62C crosslinked at 200°C in air and pyrolyzed at 1000, 1400 and 1700°C in argon (1K/min)

The chemical compositions and empirical formula of the ceramic materials obtained upon pyrolysis at 1000, 1400 and 1700°C are summarized in Table 1. The phase composition is calculated based on Si-O, and Si-C bonding and on the presence of residual free carbon[16]. The significant amount of oxygen at 1000 and 1400°C comes from the polysiloxane structure. At these temperatures, since the material is amorphous, the phase composition can only be expressed as SiOC and free carbon phases. Crystallization at 1700°C occurs by a carbothermal reduction and a phase separation between SiO_2 and carbon[17] expressed by equation (1), leading to a mixture of SiC, SiO_2 and free carbon.

$$SiO_2(s) + 3C\ (s) \rightarrow SiC\ (s) + 2CO(g) \tag{1}$$
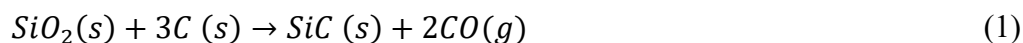
From 1000 to 1400°C, the elemental composition of the Silres H62C-c is similar. The presence of excess of carbon was proven using Raman spectroscopy with the detection of D and G bands (data are not reported in this paper). At 1700°C, oxygen content reduces significantly from 24 to 1.6 at %, confirming the occurrence of the carboreduction reaction. Since silicon is the limiting reagent, the free carbon phase is still present in the final ceramic.

Temperature of pyrolysis	Formula	Elemental composition (at. %)				Phase composition (wt. %)			
		Si	O	C	H	SiOC	SiC	SiO$_2$	C$_{free}$
1000°C	SiC$_{2.30}$O$_{1.14}$	21.8	25	50.3	< 0.01	69.6	-	-	30.4
1400°C	SiC$_{2.27}$O$_{1.04}$	23.2	24.1	52.7	N/A	70.1	-	-	29.9
1700°C	SiC$_{1.61}$O$_{0.04}$	37.7	1.6	60.7	N/A	-	81.7	2.5	15.8

Table 1 Elemental analysis of pyrolysed silres H62C-c at 1000°C, 1400C and 1700°C in flowing argon (IGA and ICP analyses)

The ceramic samples prepared upon pyrolysis at 1400 and 1700°C were investigated with respect to their microstructure by TEM, Fig. 4. The ceramic prepared at 1400°C (Fig. 4, A) showed a homogeneous microstructure. HRTEM imaging (Fig. 4, B) reveals mainly an amorphous material but also the presence of few nanometer-sized crystallites and areas constituted by turbostratic carbon, which confirms the results from chemical analyses. The sample prepared at 1700°C observed at a low magnification exhibits a two-phase microstructure, Fig. 4, C. The dark phase has a wormy morphology, is polycrystalline and some individual grains are twinned. The bright grey phase is amorphous and enriched in carbon a (assessed by STEM/HAADF/EDS, data is not reported in this paper). HRTEM imaging (Fig. 4, D) shows an interface between the amorphous and crystalline phases. The right-hand side inset in Fig. 4, D shows Fast Fourier Transformation (FFT) of the image acquired on the crystalline phase. Itis analogous to a diffraction picture and is characteristic of the 3C-SiC polytype.
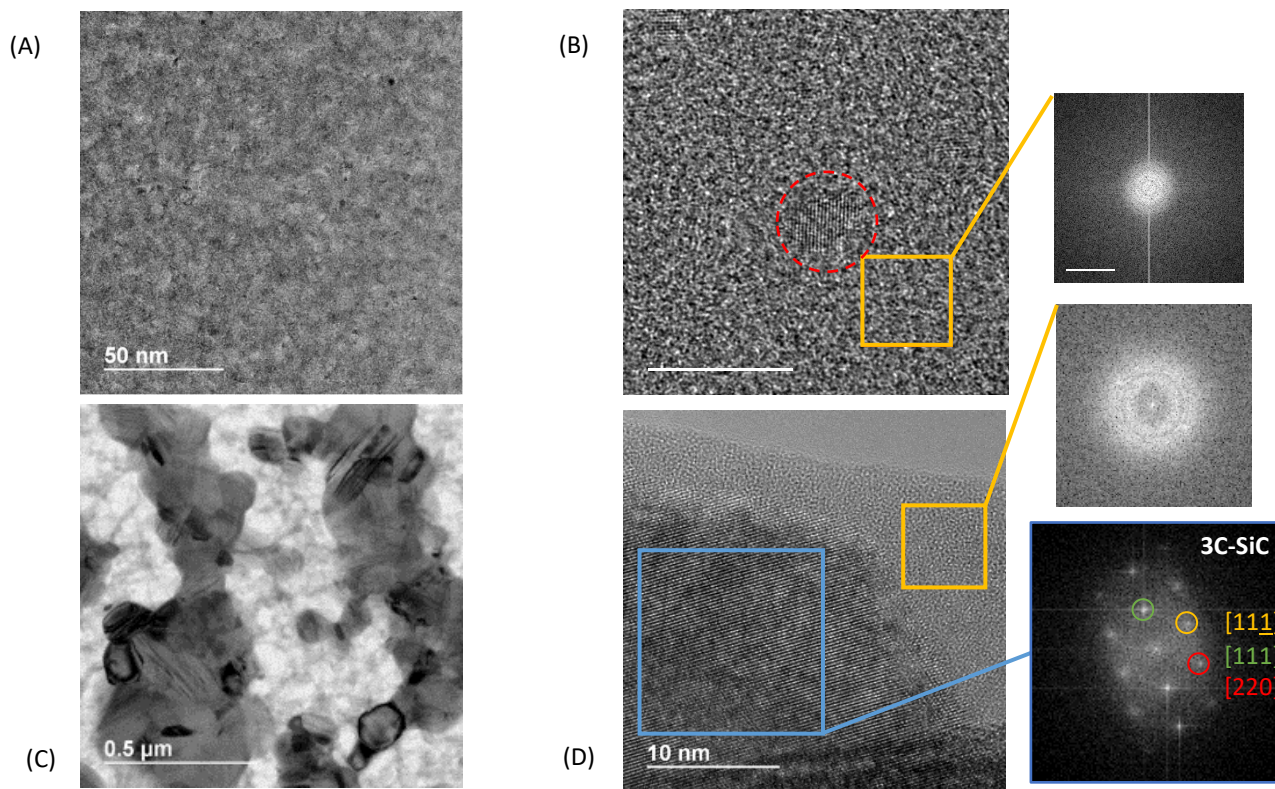

Fig. 4 HRTEM of H62C pyrolyzed in argon at (A), (B) 1400°C and (C), (D) 1700°C.

4.2 Development of PDC photocurable formulation

Effect of photoinitiators on cured thickness

The cured thickness for eight PDC-F1 formulations blended with four different PIs at 1 mol.% and 2 mol.% were plotted in Fig. 5. The formulations have a high reactivity as the layer thickness measured is beyond the target of 200 μm. A 2 mol.% of PI in the resin exhibits a lower layer thickness compare to 1 mol.% of PI. The formulation including 2 mol.% of PI-819 lead to layer thickness close to the target of 200 μm. Having a high amount of PIs as 2 mol.% in the PDC formulation leads to fast curing on the top of the layer, limiting the UV penetration depth and the cured thickness. In addition, these formulations are subject to dark curing.

As it stands, the PDC-F1 formulations are not suitable to cure thickness between 100 and 200 µm. However, the formulation with the PI-819 appears to have a better lateral resolution and a homogeneous depth of polymer conversed.
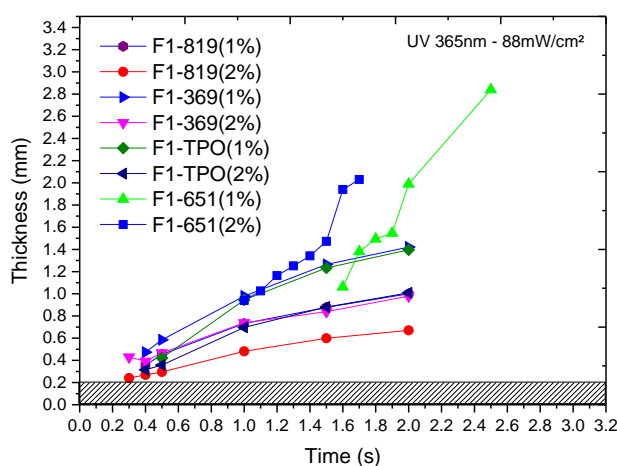

Fig. 5 Polymerized thickness versus curing time of UV light (365nm) with 88mW/cm² irradiance. Effect of type and rate of photoinitiator (expressed in mol%) for formulation PDC-F1.

Effect of photoabsorber

UV-light photoabsorbers (PA) were blended to the PDC-F1 formulation containing PI-819. The PI-819 content is fixed at 0.6 mol.% to avoid dark curing. Active di-functional acrylate solvent (PEGDA) was added to dissolve the organic dye (PDC-F2). The effects of the four photo-absorbers are presented in Fig. 6, a. The presence of photoabsorber, even at low content (0.1 mol.%), reduces by 60% to 80% the cured thickness. The cured thickness at 0.1 mol.% are therefore beyond the target thickness, except for the BBOT formulation for a curing duration of 1s.

BBOT is a luminescent dye. Its emission spectra[13] overlaps the absorption one of the photoinitiator PI-819[18]. Parts printed by stereolithography with the formulation PDC-F2 containing the BBOT photoabsorber have shown a loss of resolution. The photon reemission of the BBOT may initiate PI and lead to lateral over-curing.

Cu(II)PC is an organic dye which has a limited dissolution in PEGDA.

Using Sudan I at a minimum amount fixed to 0.22 mol.% F2 is sufficient to decrease the penetration depth and leads to a thickness under 200 µm (Fig. 6, b). Free objects will be printed with the formulation PDC-F2 with Sudan I. The manufacturing of parts are reported in paragraph 4.4.
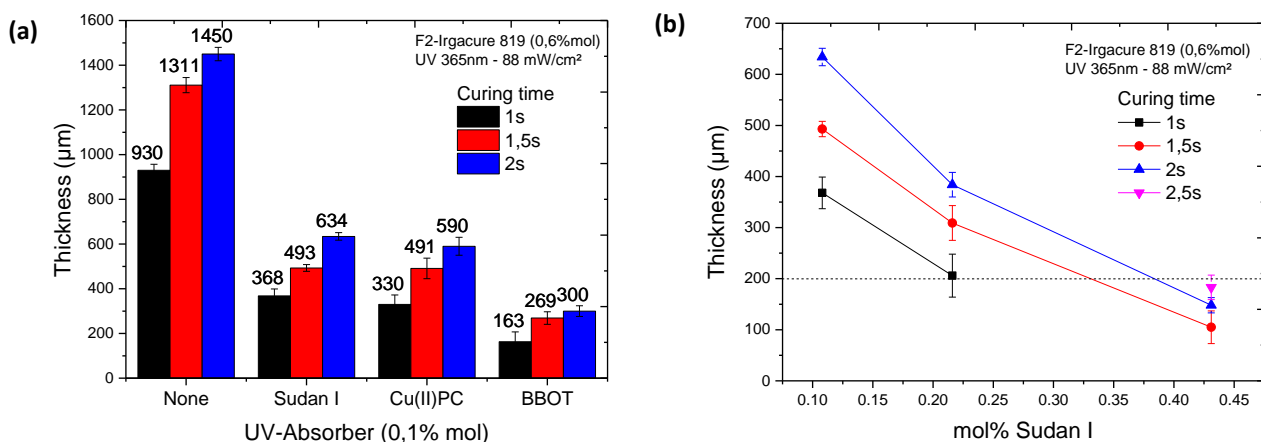
Fig. 6 Polymerized thickness versus (a) type of photoabsorber at isomolar concentration (0.1 mol.%) and (b) versus molar concentration of photoabsorber Sudan I with formulation F2 (PI-819 at 0.6 mol.%) at 88 mW/cm² irradiance.

4.3 Polymerization kinetics

Effect of preceramic polymer content and irradiance

In PDC photocurable formulations, a high concentration of Silres H62C is needed to reach high ceramic yields after pyrolysis and a sufficient acrylate monomer concentration to confer a mechanical strength during the printing step. To quantify the effect of the H62C content, the polymerization profiles of F2 resins containing between 25 and 75 wt.% of acrylates including PI-819 (0.6 mol.% relative to acrylate amount), were recorded at an irradiance of 88 mW/cm² (Fig. 7, a). The monomer concentration strongly affects the polymerization kinetics. The polymerization rate and the final conversion of the acrylate groups are detailed in Table 2.

Silres H62C slightly absorbs the 365 nm UV light (assessed by UV Spectroscopy, data are not reported in this paper), however the kinetics of formulation with 25 wt. % of monomer shows a polymerization rate of 0.8 s^{-1} and is 2 to 8 times slower compared to the literature[19]. This formulation is still considered as a fast polymerization system with a 88 mW/cm² fixed irradiance value.
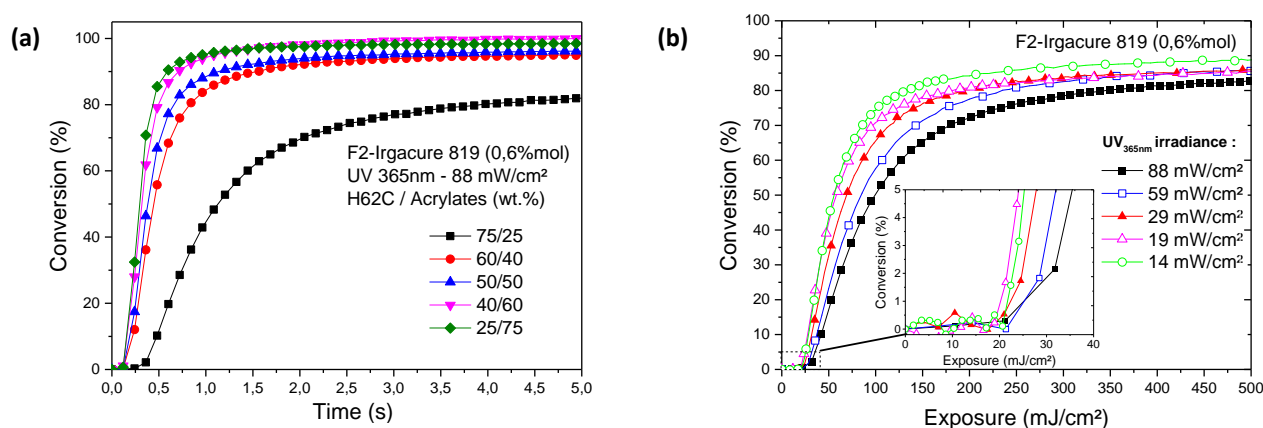

Fig. 7 Polymerization profile of the F2 with 0.6 mol.% of PI-819 relative to acrylate amount (a) effect of monomer concentration and (b) effect of irradiance

Monomer content (wt. %)	$\left(\dfrac{Rp}{[M]_0}\right)_{max}$ (s^{-1})	Final conversion (after 30s irradiation) (%)
75	3.1	100
60	2.8	99
50	2.4	97
40	1.9	96
25	0.8	88.5

Table 2 Effect of the monomer concentration on the polymerization rate for the F2 resin with 0.6 mol.% of PI-819 at 88 mW/cm² irradiance

The effect of irradiance between 14 and 88 mW/cm² was investigated to characterize kinetics of photopolymerisation. The conversion versus exposure is plotted in Fig. 7, b. The polymerization starts at an exposure around 20 mJ/cm². For an irradiance of 88 mW/cm², this exposure value corresponds to an induction time of 227 ms. The irradiance value affects, however, the final conversion rate.

During the SLA process, the resin is directly in contact with the ambient air. As oxygen inhibits polymerization, the induction period should be longer. A high irradiance value (88 mW/cm²) usually overcomes inhibition issues.

4.4 Stereolithography and chemical analysis

Parts with a grid shape (1.5 mm wall thickness and 3 mm height) were printed with the layer-wise SLA process based on the PDC-F2 formulation containing 0.4 mol. % of Sudan I and PI-819 at 0.6 mol.%. Printed parts were cross-linked in air at 200°C and pyrolysed in argon at 1000°C. The Fig. 8, a, b, c, d depicts the structures at each steps of the process. The linear shrinkage after pyrolysis is 25% and the weight loss is 53 wt. %. No visible deformation, delamination or cracks of the structures were observed. The high weight loss corresponds to the ceramization of the Silres H62C compound and integrates also the burnout step of the photocurable resin. The free carbon content measured from the STEM/EDX in the part is 45.6 wt. %. This value, higher than the one for the pure Silres H62C (30.4 wt. %) confirms the presence of carbonaceous residues from the partial degradation of the resin.
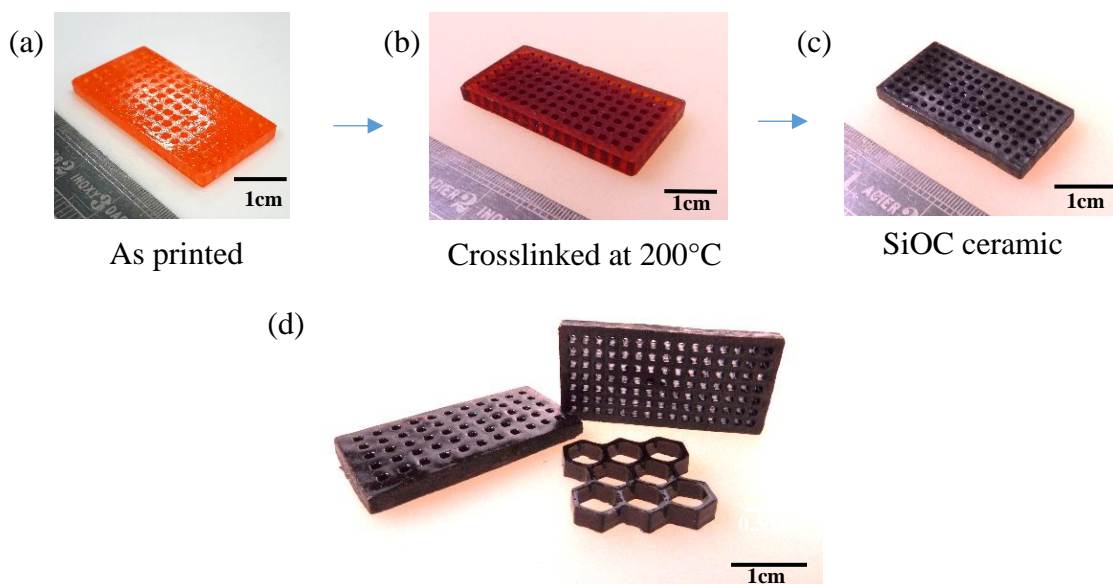

(a) As printed (b) Crosslinked at 200°C (c) SiOC ceramic (d)

Fig. 8 Pictures of (a) green body with the PDC-F2 formulation with Sudan I printed with 88mW/cm² irradiance (b) cured in air at 200°C and (c, d) pyrolyzed at 1000°C in argon atmosphere.

Conclusions

The commercial methylphenylvinylhydrogen polysiloxane Silres H62C enables to obtain, at 1000°C in argon, an amorphous ceramic material which is chemically composed of $SiO_{2.3}C_{1.14}$. After a carboreduction step at 1700°C in argon, the oxycarbide ceramic presents an amorphous carbon-rich phase and a crystalline 3C-SiC phase. The final material composition is SiC 81.7 wt. %, SiO_2 2.5 wt. % and C_{free} 15.8 wt. %. This polysiloxane has a high C_{free} content compared to polycarbosilane. As an example, SMP-10 Starfire Systems reaches about 2 wt. % in C_{free} at 1700°C (argon, not reported in this paper) with a composition close to SiC.

A photocurable formulation filled with a high content of Silres H62C (75 wt. %) was developed. It ensures a high ceramic yield after pyrolysis (47 wt. %). To provide a high resolution printed part, an organic photoabsorber is added (0.4 wt. % of Sudan I) to the PDC-photocurable formulation. Even with a high content of Silres H62C, the formulation shows a fast curing behaviour. The assessment of kinetics properties showed a low polymerization energy (20 mJ/cm²) and a high polymerization rate (0.8 s^{-1}).

The development of the photocurable formulation enables to print parts using the SLA DLP printing technology. Thermal treatment leaded to a 47 wt. % of weight loss and to a 25% linear shrinkage. The chemical analysis after pyrolysis showed an increase of carbon content explained by the partial degradation of the resin.

References

(1) Travitzky, N.; Bonet, A.; Dermeik, B.; Fey, T.; Filbert-Demut, I.; Schlier, L.; Schlordt, T.; Greil, P. Additive Manufacturing of Ceramic-Based Materials: Additive Manufacturing of Ceramic-Based Materials. *Advanced Engineering Materials* **2014**, *16* (6), 729–754. https://doi.org/10.1002/adem.201400097.

(2) Badev, A.; Abouliatim, Y.; Chartier, T.; Lecamp, L.; Lebaudy, P.; Chaput, C.; Delage, C. Photopolymerization Kinetics of a Polyether Acrylate in the Presence of Ceramic Fillers Used in Stereolithography. *Journal of Photochemistry and Photobiology A: Chemistry* **2011**, *222* (1), 117–122. https://doi.org/10.1016/j.jphotochem.2011.05.010.

(3) Colombo, P.; Mera, G.; Riedel, R.; Sorarù, G. D. Polymer-Derived Ceramics: 40 Years of Research and Innovation in Advanced Ceramics: Polymer-Derived Ceramics. *Journal of the American Ceramic Society* **2010**, *93* (7), 1805–1837. https://doi.org/10.1111/j.1551-2916.2010.03876.x.

(4) Friedel, T.; Travitzky, N.; Niebling, F.; Scheffler, M.; Greil, P. Fabrication of Polymer Derived Ceramic Parts by Selective Laser Curing. *Journal of the European Ceramic Society* **2005**, *25* (2–3), 193–197. https://doi.org/10.1016/j.jeurceramsoc.2004.07.017.

(5) Mott, M.; Evans, J. R. Solid Freeforming of Silicon Carbide by Inkjet Printing Using a Polymeric Precursor. *Journal of the American Ceramic Society* **2001**, *84* (2), 307–13.

(6) Zanchetta, E.; Cattaldo, M.; Franchin, G.; Schwentenwein, M.; Homa, J.; Brusatin, G.; Colombo, P. Stereolithography of SiOC Ceramic Microcomponents. *Advanced Materials* **2016**, *28* (2), 370–376. https://doi.org/10.1002/adma.201503470.

(7) Schmidt, J.; Colombo, P. Digital Light Processing of Ceramic Components from Polysiloxanes. *Journal of the European Ceramic Society* **2018**, *38* (1), 57–66. https://doi.org/10.1016/j.jeurceramsoc.2017.07.033.

(8) C. Eckel, Z.; Zhou, C.; Martin, J. H.; Jacobsen, A. J.; Carter, W. B.; Schaedler, T. A. Additive Manufacturing of Polymer-Derived Ceramics. *Science* **2016**, *351* (6268), 58–62. https://doi.org/10.1126/science.aad2087.

(9) Brinckmann, S. A.; Patra, N.; Yao, J.; Ware, T. H.; Frick, C. P.; Fertig, R. S. Stereolithography of SiOC Polymer-Derived Ceramics Filled with SiC Micronwhiskers. *Advanced Engineering Materials* **2018**, *20* (11), 1800593. https://doi.org/10.1002/adem.201800593.

(10) de Hazan, Y.; Penner, D. SiC and SiOC Ceramic Articles Produced by Stereolithography of Acrylate Modified Polycarbosilane Systems. *Journal of the European Ceramic Society* **2017**, *37* (16), 5205–5212. https://doi.org/10.1016/j.jeurceramsoc.2017.03.021.

(11) Li, S.; Duan, W.; Zhao, T.; Han, W.; Wang, L.; Dou, R.; Wang, G. The Fabrication of SiBCN Ceramic Components from Preceramic Polymers by Digital Light Processing (DLP) 3D Printing Technology. *Journal of the European Ceramic Society* **2018**. https://doi.org/10.1016/j.jeurceramsoc.2018.06.046.

(12) Wang, X.; Schmidt, F.; Hanaor, D.; Kamm, P. H.; Li, S.; Gurlo, A. Additive Manufacturing of Ceramics from Preceramic Polymers: A Versatile Stereolithographic Approach Assisted by Thiol-Ene Click Chemistry. *Additive Manufacturing* **2019**, *27*, 80–90. https://doi.org/10.1016/j.addma.2019.02.012.

(13) Wang, F.; Chong, Y.; Wang, F.; He, C. Photopolymer Resins for Luminescent Three-Dimensional Printing: ARTICLE. *Journal of Applied Polymer Science* **2017**, *134* (32), 44988. https://doi.org/10.1002/app.44988.

(14) Matthews, S.; J. Edirisinghe, M.; Folkes, M. J. Effect of Prepyrolysis Heat Treatment on the Preparation of Silicon Carbide from a Polycarbosilane Precursor. *Ceramics International* **1999**, *25*, 49–60. https://doi.org/10.1016/S0272-8842(97)00088-6.

(15) Pujar, V. V.; Cawley, J. D. Effect of Stacking Faults on the X-Ray Diffraction Profiles of β-SiC Powders. *Journal of the American Ceramic Society* **1995**, *78* (3), 774–782. https://doi.org/10.1111/j.1151-2916.1995.tb08246.x.

(16) Martínez-Crespiera, S.; Ionescu, E.; Kleebe, H.-J.; Riedel, R. Pressureless Synthesis of Fully Dense and Crack-Free SiOC Bulk Ceramics via Photo-Crosslinking and Pyrolysis of a Polysiloxane. *Journal of the European Ceramic Society* **2011**, *31* (5), 913–919. https://doi.org/10.1016/j.jeurceramsoc.2010.11.019.

(17) Saha, A.; Raj, R. Crystallization Maps for SiCO Amorphous Ceramics. *Journal of the American Ceramic Society* **2007**, *90* (2), 578–583. https://doi.org/10.1111/j.1551-2916.2006.01423.x.

(18) Ciba Specialty Chemicals Inc. Photoinitiators for UV Curing - Key Products Selection Guide 2003.

(19) Studer, K.; Decker, C.; Beck, E.; Schwalm, R. Overcoming Oxygen Inhibition in UV-Curing of Acrylate Coatings by Carbon Dioxide Inerting, Part I. *Progress in Organic Coatings* **2003**, *48* (1), 92–100. https://doi.org/10.1016/S0300-9440(03)00120-6.